BULLETIN OF THE POLISH ACADEMY OF SCIENCES
TECHNICAL SCIENCES, Vol. 69(1), 2021, Article number: e136039
DOI: 10.24425/bpasts.2021.136039

CIVIL ENGINEERING

Accuracy assessment of linear elasticity solution for interaction of cylindrical tank with subsoil

Paweł Marek LEWIŃSKI*

Building Research Institute, ul. Filtrowa 1, 00-611 Warszawa, Poland

Abstract. The subject of this paper is an assessment of the accuracy of a solution based on the linear theory of elasticity describing the interaction of a cylindrical reinforced concrete tank with the subsoil. The subsoil was modelled in the form of an elastic half-space and Winkler springs. The behaviour of the shell structure of the RC cylindrical tank, and particularly of the ground slab interacting with the subsoil, depends largely on the distribution of the reactions on the foundation surface. An analysis of this structure with the shell fixed in a circular ground slab was carried out taking into consideration the elastic half-space model using the Gorbunov-Posadov approach and, for comparison, the two-parameter Winkler model. Although the results for both subsoil models proved to be divergent, the conclusions that follow the accuracy assessment of a solution based on the theory of elasticity are fairly important for engineering practice.

Key words: RC tank; cylindrical tank; soil-structure interaction; theory of elasticity; Winkler model.

1. Introduction

The design of reinforced concrete structures for retaining liquids is a complex task, demanding a wide range of specialized knowledge and adequate experience. Ground settlement leading to the deformation and cracking of RC tanks may cause severe damage; therefore, special attention is paid to this problem. A number of papers have focused on the effects of loads leading to deformations connected with the reaction of the subsoil on the ground slab as a result of the interaction between the subsoil and the structure. The behaviour of the shell structures of RC cylindrical tanks, and particularly of the ground slab interacting with the subsoil, depends largely on the distribution of the subsoil reactions on the foundation surface. The distribution of the subsoil reaction on the ground slab in such a structure as a tank has a significant impact on the behaviour of not only the slab itself, but also the interacting shell structure. The discussed interactive reactions were described using different models of subsoil, such as the Winkler model, multi-parameter models and the hypothesis of the elastic half-space. In the design calculations of the structure, elastic subsoil models are usually assumed, allowing for the superposition of the actions on the structure. The subject of this paper is the assessment of the accuracy of a solution based on the linear theory of elasticity describing the interaction of cylindrical RC tanks with the subsoil defined in the form of an elastic half-space and, for comparison, the Winkler model. Elastic interactions between the tank structure and the soil base have been the subject of many hitherto published papers. The utilization of the present model, based on the theory of linear elasticity, was initiated by Borowicka [1] and then developed by Gorbunov-Posadov [2].

Within the framework of the application of the elastic half-space model for the description of soil-structure interaction, there is lack of closed solutions for many boundary problems. Thus, it is necessary to use different approximated methods and trace their accuracy. Some partial results for the proposed model in the case of cylindrical water tanks with linearly varying wall thickness were presented by the author and Rak at the PCM-CMM-2015 conference [3], while the interaction of such structures with subsoil under thermal gradient conditions was presented at the XXVIII R-S-P TFoCE Seminar [4]. Lewiński and Rak [3, 4] employed an analytical approach based on the Gorbunov-Posadov method using the convergence control of the power series of the solution. Besides the analytical solution applied further below, variational formulations and numerical approaches are also used, based on the finite element method and other methods. In the case of analytical approaches, the methods supported by energy formulations are often used, leading to approximated solutions. The assumed approach gives the advantage of being relatively simple and exact, in relation to common modelling methods. In the available literature, however, this method has not been widely used. Kukreti, Zaman and Issa [5] utilized the principle of minimum potential energy for the determination of the coefficients of the function describing the ground slab deflection. In the case of a cylindrical tank of varying wall thickness supported on a circular ground slab, Kukreti and Siddiqi [6] used the quadrature method, i.e., an approximated approach, involving polynomial functions with weights at selected points. The approaches presented in some papers favour Hankel transforms and the Bessel function series (see Hemsley [7, 8]) or numerical methods (Melerski [9], Horvath and Colasanti [10], el Mezaini [11], Mistríková and Jendželovský [12]), which lead to complicated algorithms or approximated results. Therefore, a more detailed examination of the impact of approximation of a solution, based on the linear elasticity, on the accuracy of determining the response of a RC cylindrical tank-subsoil system was considered necessary.

*e-mail: p.lewinski@itb.pl

Manuscript submitted 2020-07-06, revised 2020-09-08, initially accepted for publication 2020-10-12, published in February 2021

2. Analysis of soil-structure interaction

For analytical purposes, it can be assumed that the slab perfectly adheres to the surface of the subsoil, which has the properties of the elastic half-space. The slab acts on the subsoil without friction and perfectly adheres to it even when there is a tension between the slab and the substrate (in the case of concrete tanks, this phenomenon is not observed). In order to attain the solution for an elastic and isotropic half-space loaded on a certain domain of the limiting plane in a perpendicular way, the influence surface is used (the Green function), i.e., by using the Boussinesq solution obtained for arbitrarily located vertical force P acting on the isotropic half-space [1, 2]. According to this solution, the vertical displacement of the limiting plain ($z = 0$) amounts to:

$$\upsilon\big|_{z=0} = \frac{P\left(1-\nu_0^2\right)}{\pi E_0 r}, \tag{1}$$

where E_0 and ν_0 are the modulus of elasticity and Poisson ratio of the elastic half-space, respectively, while r is the distance of the considered point from the point of the application of concentrated force P. Considering the loading of such a half-space by the pressure transmitted through a circular slab in a perpendicular way, one can assume that the axi-symmetric loading $p(r)$ operates on it – at the same time, this is a function describing the half-space reaction acting on the slab.

Let us introduce non-dimensional variables: ρ, $\bar{\rho}$, α and the angle χ such that:

ρ – non-dimensional distance from the centre of the slab to the point A of the surface of the subsoil, in which the displacement is evaluated ($\rho = r/R$, where r – real distance, R – slab radius; (see Fig. 1a)),

$\bar{\rho}$ – non-dimensional distance from the slab centre to the point B of the application of the infinitesimal load ($\bar{\rho} = t/R$, where t – the distance to the point B; (Fig. 1a)),

α – non-dimensional radius of loading q, $\alpha = a/R$, where: a – loading radius (see Fig. 1b),

χ – angle OBA and the parameter of integration; (Fig. 1a).

The Green function was integrated over the surface of the circular slab. The elastic subsidence of half-space, $\upsilon(\rho)$, from load $p(\rho)$ transmitted by the circular slab (see [13]), can be given in the form:

$$\upsilon(\rho) = \frac{4\left(1-\nu_0^2\right)R}{\pi E_0}\left[\frac{1}{\rho}\int_0^{\rho} p(\bar{\rho})\bar{\rho}\int_0^{\pi/2}\frac{\mathrm{d}\chi}{\sqrt{1-\left(\frac{\bar{\rho}}{\rho}\right)^2\sin^2\chi}}\,\mathrm{d}\bar{\rho} + \int_{\rho}^{\alpha} p(\bar{\rho})\int_0^{\pi/2}\frac{\mathrm{d}\chi}{\sqrt{1-\left(\frac{\rho}{\bar{\rho}}\right)^2\sin^2\chi}}\,\mathrm{d}\bar{\rho}\right]. \tag{2}$$

As the subsoil reaction on the slab acts on its entire bottom surface, parameter $\alpha = 1$ ($a = R$). The differential equation of the circular slab resting on the elastic half-space and subjected to loading q, uniformly distributed on the surface of the circle of radius a, takes the form:

$$\frac{\mathrm{d}^4 w}{\mathrm{d}\rho^4} + \frac{2}{\rho}\cdot\frac{\mathrm{d}^3 w}{\mathrm{d}\rho^3} - \frac{1}{\rho^2}\cdot\frac{\mathrm{d}^2 w}{\mathrm{d}\rho^2} + \frac{1}{\rho^3}\cdot\frac{\mathrm{d}w}{\mathrm{d}\rho} = \frac{R^4}{D}\left[q - p(\rho)\right], \tag{3}$$

where D is the bending stiffness of the slab. The displacements of the surface of the elastic half-space and the displacements of the slab must be identically equal: $\upsilon(\rho) \equiv w(\rho)$.

Function $p(\rho)$ of the interaction between the slab and the elastic half-space can be assumed in the form of the series:

$$p(\rho) = \sum_{n=0}^{\infty} a_{2n}\rho^{2n}. \tag{4}$$

In order to evaluate the integral of Eq. (3), at first a homogeneous equation can be considered. Its solution constitutes the function:

$$w_o = C_1\rho^2\ln\rho + C_2\rho^2 + C_3\ln\rho + C_4, \tag{5}$$

where C_i, $i = 1 \ldots 4$ are the constants of integration.

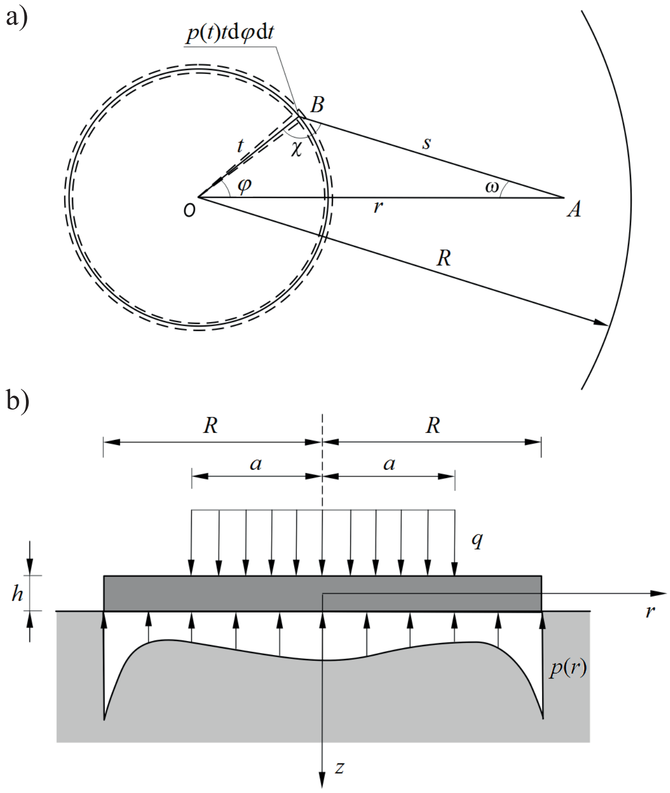

Fig. 1. The loading schemes of the circular slab on elastic half-space. Description of notations – in the text; s – distance from the point A to the point B of the application of infinitesimal load $p(t)t\mathrm{d}\varphi\mathrm{d}t$

The particular integral of Eq. (3) can be sought in the form:

$$w_s = \sum_{n=2}^{\infty} A_{2n}\rho^{2n}. \tag{6}$$

Coefficients A_{2n} may be expressed by components a_{2n} of a series (4) by substituting this series to Eq. (3) and comparing the components of identical powers. The full solution can be obtained by adding the particular integral to Eq. (5). Eventually, the slab deflection in the area (which is denoted by index I) of the action of loading q is expressed by equation:

$$\begin{aligned} w_I &= C_{1,I}\rho^2\ln\rho + C_{2,I}\rho^2 + C_{3,I}\ln\rho + C_{4,I} + \\ &+ \frac{R^4}{64D}(q-a_0)\rho^4 - \frac{R^4}{16D}\sum_{n=1}^{\infty}\frac{a_{2n}}{(n+2)^2(n+1)^2}\rho^{2n+4}. \end{aligned} \tag{7}$$

Equation (7) is also valid in the unloaded area (of index II) – by the substitution $q = 0$. Constants C_1, ..., C_4 are determined from the conditions in the centre and at the boundaries of the slab. In order to solve the problem, the infinite system of equations is replaced by a system of N equations. Limiting the expansions of infinite series in expressions (4), (6) and (7) to the order of approximation of N terms for each series, substituting the expression of interaction function (4) into the equation of the vertical displacement of the subsoil surface (2), expressing both elliptic integrals by the hypergeometric series, and then performing the multiplication and integration of the series, one can get the equation for the vertical displacements of the half-space on the area undergoing axi-symmetrical loading also in the form of a power series, as below.

$$\begin{aligned} \upsilon(\rho) &= \\ &= \frac{2(1-\nu_0^2)R}{E_0}\left\{\sum_{n=0}^{N}\sum_{m=0}^{N}\left[\frac{\prod_{k=0}^{m}(2k-1)}{2^m m!}\right]^2\frac{a_{2n}}{2n-2m+1}\rho^{2m}\right\} \end{aligned} \tag{8}$$

By identifying $\upsilon(\rho) \equiv w(\rho)$, the coefficients of the series at the equal powers of ρ in expressions (7) and (8) can be compared, the beginning from the second, which leads to a set of N algebraic equations, allowing for the evaluation of coefficients a_{2n}. To this set of algebraic equations, the equilibrium equation of the loads acting on the slab should be added first. This equation can be received in two ways: by the integration of the interaction function $p(\rho)$ or from the boundary condition describing the imposition of zero value of the shear force around the edge of the plate: $Q_r(1) = 0$. The first method is used herein (the assumption of the axi-symmetrical loading of the plate only on the area of the circle of radius a is used) and the result of the integration takes the form:

$$\begin{aligned} q\int_0^{2\pi}\int_0^{a}\bar\rho\,\mathrm{d}\bar\rho\,\mathrm{d}\varphi &= \int_0^{2\pi}\int_0^{1}\bar\rho p(\bar\rho)\,\mathrm{d}\bar\rho\,\mathrm{d}\varphi = \\ &= \int_0^{2\pi}\int_0^{1}\left(\sum_{n=0}^{N}a_{2n}\bar\rho^{2n+1}\right)\mathrm{d}\bar\rho\,\mathrm{d}\varphi. \end{aligned} \tag{9}$$

After the bilateral integration of Eq. (9), the first equilibrium equation can be received:

$$q\frac{a^2}{R^2} = \sum_{n=0}^{N}\frac{a_{2n}}{1+n}. \tag{10}$$

In practical calculations, the convergence of the solution should be examined and number N can be evaluated. Around the edge of the slab, in the circle surrounding radius $r = R$, stress concentration in the subbase can be encountered (as it is a contact problem) and, therefore, in the case of series (4) for $N \to \infty$, function value $p(1)$ can pursue infinity. Thus, if this function were expressed by the infinite power series, this would have been divergent at this point. Next, the case of the equilibrium of stress resultants on the slab circumference should be considered: the radial bending moments, as well as radial, shear and vertical edge forces through the formulation of proper boundary conditions.

In order to perform the comparative calculations of the ground slab of the tank, the model of the circular slab resting on the two-parameter Winkler subbase (taking into account the vertical subbase reaction modulus $k_1 = K_z$ and the horizontal one $k_2 = K_t$) was used herein (see [14]). The biharmonic differential equation applicable in this case can first be solved as homogeneous and can be transformed into the product of two modified Bessel equations. The general solution of the non-homogeneous equation takes the form:

$$w(\rho) = \frac{q}{K_v} + C_1\mathrm{ber}(\kappa\rho, \psi) + C_2\mathrm{bei}(\kappa\rho, \psi), \tag{11}$$

where the following denotations are used:

$$\psi = \frac{1}{2}\arccos\left(\frac{\gamma}{\delta}\right), \;\; \kappa = \sqrt{\delta} = a\sqrt[4]{\frac{K_z}{D}} \;\text{ and }\; \gamma = \frac{K_t h^2 a^2}{8D}.$$

In the case of load q uniformly distributed on the circular surface with radius a, a vertical deflection at the centre of the circle can be obtained as a result of the Green function integration (see Eq. (1)):

$$w(0) = \frac{2(1-\nu_0^2)qa}{E_0}. \tag{12}$$

When pressing a rigid cylindrical indenter with a flat end and radius a into the elastic half-space plane and replacing the indenter force P by the expression $q\cdot\pi a^2$, the formula for vertical deflection takes the form:

$$w = \frac{\pi(1-\nu_0^2)qa}{2E_0}. \tag{13}$$

3. Problem solution and accuracy estimation

Based on the above-described algorithm, the behaviour of the RC cylindrical tank subjected to different variants of axi-symmetrical load was analysed taking into account two substrate models, i.e., an elastic half-space and two-parameter Winkler models. The structure of a tank with sufficiently high tensile strength is considered herein, so it was assumed that the concrete of the tank, due to the required tightness, is uncracked or cracked to such a small extent that the tensile reinforcement compensates the loss of stiffness due to cracking. Generally, the influence of the reinforcement is neglected. This allowed for the assumption that the tank's structure is made of a homogeneous, isotropic material with the elastic properties and specific weight characteristic for plain concrete. A water tank made of concrete with elasticity modulus: 31 GPa, and Poisson ratio: 0.2 was assumed, consisting of a cylindrical shell with an average radius of 7.0 m, height of $l = 5.0$ m and thickness (h) of 20 cm, joined with a circular ground slab 20 cm thick. The ground in the substrate with: $E_0 = 280$ MPa and $\nu_0 = 0.3$ was assumed. In the comparative calculations for the Winkler foundation, two subgrade moduli were determined based on Eqs. (12) and (13) and the friction coefficient. Comparing the displacements obtained from Eqs. (12) and (13) to the ratio q/C_z, the C_z coefficients were determined for both cases, which amounted to 22 MN/m^3 and 28 MN/m^3 respectively. Since the ground slab is neither completely flabby nor completely rigid, the intermediate value of the vertical Winkler coefficient $C_z = 25$ MN/m^3 was adopted. The coefficient of friction of concrete over the insulation layer $\mu = 0.2$ was assumed and, hence, the horizontal Winkler coefficient $C_t = 5$ MN/m^3 was determined. The geometry of the tank in a vertical cross-section is shown in Fig. 2. A few load variants were considered herein, taking into account hydrostatic pressure (the liquid specific weight was assumed to be 10 kN/m^3), the loading of the ground slab with the liquid ($p_v = 50$ kPa) and the dead weight of the wall per unit of the circuit: $P = \gamma_c \cdot l \cdot h = 25$ kN/m, where the specific weight of the RC structure (γ_c) was assumed as 25 kN/m^3. In order to compare objectively the results obtained with the assumption of an elastic half-space and two-parameter Winkler models, the dead weight of the slab was omitted, because the ground slab undergoes deformation due to its dead weight under construction at the concrete laying stage.

In the analysis of the soil-structure interaction of the cylindrical reservoir, axisymmetrically loaded and jointed in a monolithic way with the ground slab, the force method was used (see the textbooks [15, 16]) and the theory of boundary perturbations. The conditions of applicability of this theory in the considered case are fulfilled. According to the theory of boundary perturbations, the boundary conditions for particular hyperstatic values and for the external loading of cylindrical shell as well as ground slab were formulated. For the series describing the interaction of the ground slab with subsoil, the first $N = 8$, 20, 50, 80 and 100 terms of expansion series of interaction function $p(\rho)$ were taken into account in order to check the accuracy of the solution for the case of the elastic half-space. The results obtained for the ground slab are shown in a coordinate system with the beginning at the slab centre, while the abscissa for the shell begins at the upper edge of the cylinder. The analytical results for the cylindrical tank with a ground slab resting on the elastic half-space are compared with the solution for the slab on the subbase described by the two-parameter Winkler model. The diversified results for the vertical deflections of the ground slab under hydrostatic loading for two subsoil models: the elastic half-space (for the order of approximation $N = 8$, 20, 50, 80 and 100) and two-parameter Winkler model are shown in Fig. 3. Positive displacements are directed downwards. Different distributions of the subsoil reaction under the tank for both subsoil models are given in Fig. 4. In both cases, the shell is bent from the horizontal hydrostatic pressure of the liquid; however, the ground slab is bent from the water pressure only in the case of elastic half-space model. In case of the elastic half-space model, in contrast to the Winkler model (Fig. 4), a local unlimited increase of soil reaction is observed around the perimeter.

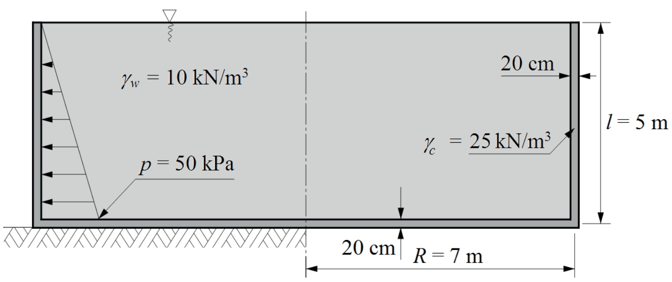

Fig. 2. The circular water tank and the horizontal hydrostatic pressure

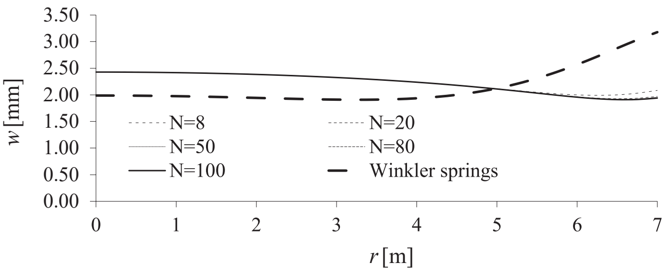

Fig. 3. Deflections of the ground slab of the tank due to hydrostatic pressure (and self-weight) for two subsoil models: elastic half-space and two-parameter Winkler model. For $N = 20$ and above, the graphs overlap

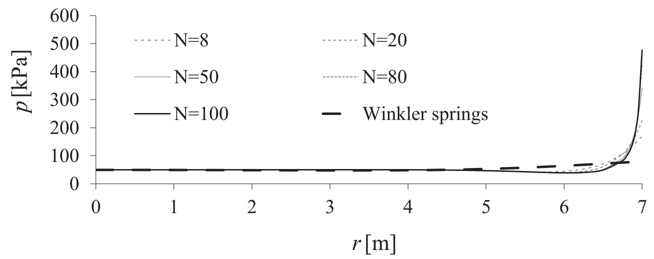

Fig. 4. Subsoil reactions under the tank due to hydrostatic pressure (and self-weight) for subsoil models: elastic half-space and two-parameter Winkler model. For $N = 80$ and above, the graphs partially overlap

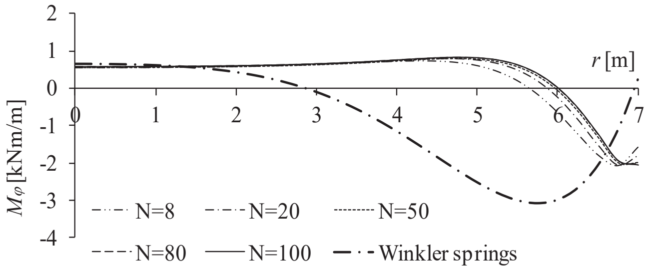

Fig. 5. Distributions of circumferential moments M_φ in the ground slab from the water pressure for the subsoil models in the form of the elastic half-space and two-parameter Winkler model. For $N = 80$ and above, the graphs overlap

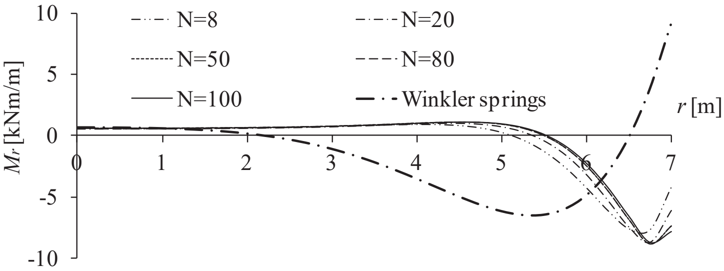

Fig. 6. Distributions of radial moments M_r in the ground slab from the water pressure for the subsoil models in the form of the elastic half-space and two-parameter Winkler model. For N=50 and above, the graphs partially overlap

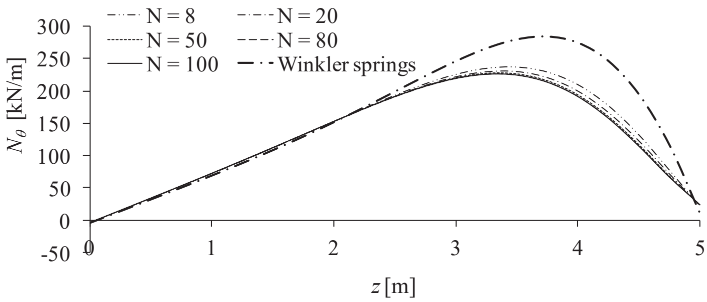

Fig. 7. Distributions of circumferential forces N_θ in the tank shell from the hydrostatic pressure for subsoil models of the elastic half-space and two-parameter Winkler model. For $N = 80$ and above, the graphs overlap

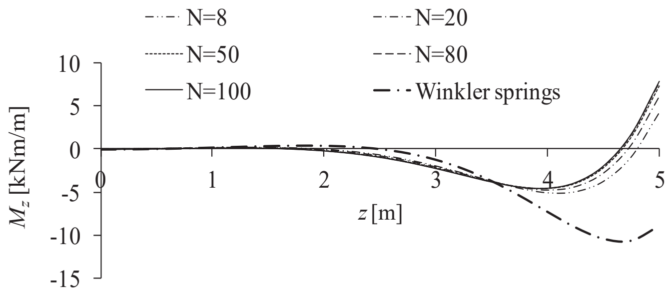

Fig. 8. Distributions of meridional moments M_z in the tank shell from the hydrostatic pressure for subsoil models of the elastic half-space and the two-parameter Winkler model. For $N = 80$ and above, the graphs overlap

The linear relationship between peripheral forces and radial displacements of tank walls causes the graph of these displacements to have a form analogous to the plot of peripheral forces (Fig. 7). A similar analogy occurs between the plot of meridional moments (Fig. 8) and circumferential moments in the tank wall, so there is no need to include charts of these displacements and moments. The convergence of the solution was investigated for different load cases; however, the present paper is focused on hydrostatic loading. By increasing the number of terms in a series describing interaction function (N) from 6 to 150, on average in decimal intervals, the differences between the results obtained for subsequent approximation orders were observed.

The convergence rate was estimated based on the meridional moment around the slab edge as a reliable value (see Figs. 6, 8 and 9), because the convergence of the displacement solution in the displacement method is very fast (see Fig. 3) and, in this case, it is not conclusive (unfortunately, in some figures the graphs for successive values of the number N overlap). The obtained results indicate the greatest sensitivity to changes in the accuracy of the solution in the vicinity of the connection of the shell with a slab. Sensitivity decreases together with distance from this point. Lack of convergence of the soil resistance function at the edge of the slab resembles the problem of a perfectly rigid cylindrical indenter pressed into the elastic half-space. As mentioned above, the anomaly is explained by the local plastification of subgrade material around the perimeter of the slab. The assessment of soil-structure interaction, however, leads to the question of uncertainty in the evaluation of

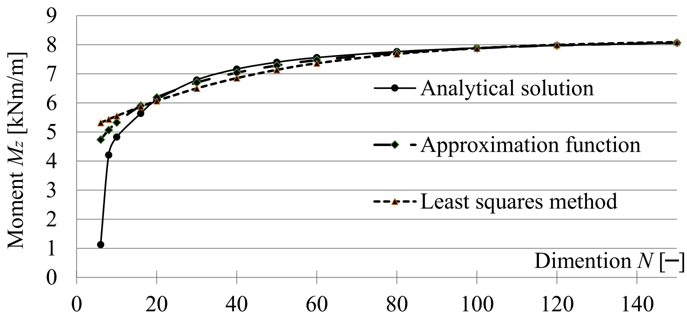

Fig. 9. The values of meridional moment $M_{z0}(N)$ around the edge of the tank shell clamped in the ground slab (equal to radial moment M_{r0} in the ground slab) from the water pressure for the subsoil model of elastic half-space in relation to the approximation order (and the approximation functions for the comparison)

structural performance and to the question asked by the author of the paper [17], namely whether a small error in the detailed assessment can lead to a large difference in the results. It was demonstrated in the cited paper that the difference in the results of strength tests of a material, which falls within the limits of uncertainty, might result in a very significant difference in the evaluation of a structure. In the problem under consideration, such uncertainty understood as dispersion attributed to a value, which is a result of the tests or calculations, is not encountered, as in the case of a typical numerical solution. However, an impact of the number of N terms in the series describing the interaction function was observed, which affects the differences between the results obtained for the subsequent approximation order. In particular, a small change of the N number from 8 to 10 terms of the considered series leads to a significant growth of meridional moment $M_{z0}(N)$ around the edge of the tank shell clamped in the ground slab from the water pressure for the subsoil model of elastic half-space (equal to the absolute value of radial moment $M_{r0}(N)$ in the ground slab) from 4.20 to 4.82 kNm/m, which denotes an increase of nearly 15%. Therefore, a thorough examination of the accuracy of the solution is necessary. A diagram given in Fig. 9 for the "Analytical solution" does not show a continuous function and was devised as a string of many particular analytical solutions. In order to facilitate the verification of the accuracy assessment of the solution based on the linear elasticity describing the interaction of the cylindrical RC tank with the subsoil, the approximation function for meridional moment $M_{z0}(N)$ was assumed in the following form:

$$M_{z0\,approx}(N) = M_{z0}(\infty)\left(1 - e^{-N/50}\right)^{1/4}, \tag{14}$$

where the meridional moment around the edge for $N = \infty$ is assumed as: $M_{z0}(\infty) \approx 8.17$ kNm/m.

The conformity assessment of the approximation function (14) and the sequence of analytical solutions may indicate the convergence of this sequence (see Fig. 9). In order, however, to adjust the approximating function to the obtained sequence of analytical solutions in a manner enabling the estimation of standard uncertainties, the linear regression method was used. In this case, it is necessary to formulate such an approximating function so that, following the appropriate transformations, the equation of a straight line can be obtained. For this purpose, the approximating function was adopted in the form:

$$M_{z0\,lsm}(N) = M_{z0}(\infty)\cdot \exp\left(-\exp(-aN - b)\right), \tag{15}$$

where a and b are straight line coefficients that can be determined by the method of linear least squares. After taking the logarithm of both sides of this equation twice, one can get an expression of type $y = ax + b$, where $x = N$, and y takes the form:

$$y = -\ln\left(-\ln\left(M_{z0}(N)/M_{z0}(\infty)\right)\right). \tag{16}$$

The method adjusts the shape of such a line to the sequence of analytical solutions so that the overall estimation error (for all solutions) is as low as possible. Both approximating functions are shown in the graph in Fig. 9. The standard uncertainty of a measurement result is the estimated standard deviation of the result. The variances in a least squares calculation: σ_a^2 and σ_b^2, the corresponding standard deviations, the coefficients of variation (defined as the ratio of standard deviation σ to the mean) and Pearson correlation coefficient r were evaluated. The calculations were carried out in order to estimate the difference between the sequence of analytical solutions of N systems of equations and the approximation function in form of Eq. (15). The low values of standard deviations and correlation coefficient r of about 0.995 allowed for a fairly positive assessment of the correlation. The comparison shown in the diagram in Fig. 9 of both approximation functions, however, represented by formulas (14) and (15), for the approximation orders (N) from 8 to 150, is given for illustration only, because in the range of N from 8 to 60, the solutions of the system of equations do not show visible convergence. Therefore, the accuracy of the solution was assessed for several approximation orders (N) from 80 to 150. The values of approximation functions according to formulas (14) and (15), and the values of approximation errors are given in Table 1. The average approximation error for Eq. (14) for $N = 80$, 100, 120, 150 is about 0.20%, while such error for Eqs. (15) and (16), evaluated based on the linear regression method for $N = 80$, 100, 120, 150, is about 0.013%. By narrowing the approximation order range in both cases, significantly lower values of standard deviations and coefficients of variation v_a and v_b were obtained, i.e., $v_a = 0.862\%$, $v_b = 1.292\%$. The Pearson correlation coefficient r of about 0.999926 obtained in this case allowed for a positive assessment of this correlation.

Table 1
Fixing moments and their estimation errors
for $N = 80$, 100, 120, 150.

Fixing Moments [kNm/m] and their Approximation Errors	Approximation Order of the Soil Reaction Function			
	$N = 80$	$N = 100$	$N = 120$	$N = 150$
$M_{z0}(N)$(analytical solution)	7.7636	7.8894	7.9744	8.0603
$M_{z0\,approx}(N)$ (Eq. (14))	7.7221	7.8783	7.9780	8.0664
Approx. error [%] for (14)	0.5345	0.1406	0.0456	0.0754
$M_{z0\,lsm}(N)$ (Eq. (15))	7.7626	7.8888	7.9764	8.0597
Approx. error [%] for (15)	0.0136	0.0083	0.0245	0.0070

The difference between the limit value of the meridional moment around the edge $\left(M_{z0}(\infty) \approx 8.170 \text{ kNm/m}\right)$ based on approximation functions (14) and (15) and the meridional moment around the edge for the first $N = 100$ terms of the expansion $\left(M_{z0}(100) \approx 7.889 \text{ kNm/m}\right)$ is not very big and is about 3.4%. The meridional moment around the edge for the first $N = 99$ terms of expansion $M_{z0}(99) \approx 7.884$ kNm/m, so the difference between the two subsequent solutions amounted to 0.65‰ < 1‰. Such accuracy, however, seems to be sufficient, as it is not possible to determine the material constants of a structure under consideration with very high accuracy due to the scatter of the results of material strength tests obtained from samples. It should be stipulated that the analysis concerned one specific task for soil-structure interaction.

4. Analysis of results

Having analysed two models of elastic subsoil, it can be stated that the assumption of the subgrade as elastic half-space in the example (regardless of number N determining the approximation order of the soil reaction function) leads to different distributions of internal forces in the tank in relation to the case of the ground slab supported on the Winkler foundation.

As a result of the analysis of the RC water tank, much smaller maximum radial displacements of the shell and substantially different bending moment diagrams were obtained compared to the Winkler model assumption. In the case of the elastic half-space model, a local nearly unrestricted increase of the substrate reaction around the circumference of the slab can be observed, unlike in the Winkler model. Lack of convergence of the soil reaction on the perimeter of the slab is justified within the framework of the theory of elasticity (in fact, local plasticizing of the substrate may occur in this area – see [18]). The differences in the moment of attachment of the shell and its sensitivity to the approximation order (N) result from the different behaviour of the ground slab, as described above. The slab resting on the elastic half-space is bent from the uniformly distributed load and edge forces, while the same structure on the Winkler foundation is bent only from the edge forces, which is manifested by the larger absolute values of the moments in the slab at the junction with the cylindrical shell. The authors of the paper [17] rightly indicate that a small error can lead to large differences in assessment. In particular, a small change of the N number from 8 to 10 terms of the considered series leads to significant growth of meridional moment $M_{z0}(N)$ around the edge of the tank shell of nearly 15%. In earlier works by various authors, based on the Gorbunov-Posadov method, the first 6 or 8 N terms of expansion series of the polynomial function for the ground reaction were assumed for the analysis, which disqualifies the results of these calculations. It can be only mentioned (without a proof of calculation) that the solution of the problem in the case of the load with a constant increase in the temperature of the shell stabilizes relatively fast, already for forty terms. In other cases, as in the case of hydrostatic pressure, comparable results are obtained more than twice as slow. Moreover, in order to adjust the approximating function to the obtained sequence of analytical solutions in a manner enabling the estimation of standard uncertainties, the linear regression method was used. For this purpose, a proper approximating function was adopted in an uncomplicated form. By narrowing the approximation order range, significantly lower values of standard deviations were obtained.

5. Conclusions

In order to verify the accuracy assessment of the solution describing the interaction of the cylindrical RC tank with the subsoil in form of the elastic half-space, simple approximation functions for meridional moment M_{z0} in the shell around the slab edge were assumed. The results of the approximation can indicate the convergence of a sequence of analytical solutions of the task and it was assessed that the difference between the limit value of the meridional moment based on the approximation functions and the meridional moment around the edge for the first 100 terms of the series expansion is not very big. Such approximation seems to be sufficient for design purposes, as it is not possible to determine the material constants of the RC tank for liquids with a very high accuracy. In order to estimate the difference between the sequence of analytical solutions of N systems of equations (obtained by equalizing vertical displacements of the elastic half-space and the ground slab), and the linear approximation function, the Pearson correlation coefficient r was evaluated. The obtained value of coefficient $r \approx 0.999926$ allowed for a positive assessment of this correlation. The analysis concerned only one specific task, so that further studies are needed in this area.

References

[1] H. Borowicka, "Pressure distribution under elastic plates", *Ing. Arch.*, X. Band, 113–125 (1939) [in German].

[2] M.I. Gorbunov-Posadov, T.A. Malikova, and V.I. Solomin, *Calculation of Structures on Elastic Foundation*, Stroyizdat, Moskva, 1984 [in Russian].

[3] P.M. Lewiński and M. Rak, "Soil-structure interaction of cylindrical water tanks with linearly varying wall thickness", *PCM-CMM-2015: 3rd Pol. Congr. Mech. & 21st Comp. Meth. Mech.*, Gdańsk, Poland, 8–11 September, 2015, vol. 2, pp. 921–922.

[4] P.M. Lewiński and M. Rak, "Soil-structure interaction of cylindrical tank of variable wall thickness under the thermal gradient conditions", *IOP Conf. Ser.: Mater. Sci. Eng.* 661, 012044 (2019)

[5] A.R. Kukreti, M.M. Zaman, and A. Issa, "Analysis of fluid storage tanks including foundation-superstructure interaction", *Appl. Math. Model.* 17, 618–631 (1993).

[6] A.R. Kukreti and Z.A. Siddiqi, "Analysis of fluid storage tanks including foundation-superstructure interaction using differential quadrature method", *Appl. Math. Model.* 21, 193–205 (1997).

[7] J.A. Hemsley (Ed.), *Design Applications of Raft Foundations*, Thomas Telford Publishing, London, 2000.

[8] J.A. Hemsley, *Elastic Analysis of Raft Foundations*, Thomas Telford Publishing, London, 1998.

[9] E.S. Melerski, *Design Analysis of Beams, Circular Plates and Cylindrical Tanks on Elastic Foundations*, Taylor & Francis Group, London, 2006.

[10] J.S. Horvath and R.J. Colasanti, "Practical subgrade model for improved soil-structure interaction analysis: Model development", *Int. J. Geomech.* 11(1), 59–64 (2011).

[11] N. el Mezaini, "Effects of soil-structure interaction on the analysis of cylindrical tanks", *Pract. Period. Struct. Des. Constr.* 11(1), 50–57 (2006).

[12] Z. Mistríková and N. Jendželovský, "Static analysis of the cylindrical tank resting on various types of subsoil", *J. Civ. Eng. Manag.* 18(5), 744–751 (2012).

[13] P. Lewiński, *Analysis of Interaction of RC Cylindrical Tanks with Subsoil*, Prace Naukowe ITB, Rozprawy, Wydawnictwa ITB, Warszawa, 2007 [in Polish].

[14] Z. Kączkowski, *Plates. Static Calculations*, Arkady, Warszawa, 2000 [in Polish].

[15] W. Flügge, *Stresses in Shells*, 2nd ed., Springer, Berlin, Heidelberg, 1973.

[16] Z.E. Mazurkiewicz and T. Lewiński (Ed.), *Thin Elastic Shells*, Oficyna Wydawnicza Politechniki Warszawskiej, Warszawa, 2004 [in Polish].

[17] E. Szewczak and A. Piekarczuk, "Performance evaluation of the construction products as a research challenge. Small error – big difference in assessment?", *Bull. Pol. Ac.: Tech. Sci.* 64(4), 675– 686 (2016).

[18] P.M. Lewiński and S. Dudziak, "Nonlinear interaction analysis of RC cylindrical tank with subsoil by adopting two kinds of constitutive models for ground and structure", *Amer. Inst. Phys.*, *AIP Conf. Proc.* 1922, 130007 (2018).